RL-TR-96-141
Final Technical Report
July 1996

FURTHER IMPROVEMENTS ON PLZT BASED MICROSTRUCTURE FOR OPTICAL SWITCHING: A HIGH EFFICIENCY ELECTRO-OPTIC GRATING SWITCH

Syracuse University

Q. Wang Song

Rome Laboratory
Air Force Materiel Command
Rome, New York

This report has been reviewed by the Rome Laboratory Public Affairs Office (PA) and is releasable to the National Technical Information Service (NTIS). At NTIS, it will be releasable to the general public, including foreign nations.

RL-TR- 96-141 has been reviewed and is approved for publication.

APPROVED:

REBECCA J. BUSSJAGER
Project Engineer

FOR THE COMMANDER:

GARY D. BARMORE, Major, USAF
Deputy Directory
Surveillance & Photonics

If your address has changed or if you wish to be removed from the Rome Laboratory mailing list, or if the addressee is no longer employed by your organization, please notify Rome Laboratory/ (OCPA), Rome NY 13441. This will assist us in maintaining a current mailing list.

Do not return copies of this report unless contractual obligations or notices on a specific document require that it be returned.

REPORT DOCUMENTATION PAGE

Form Approved
OMB No. 0704-0188

1. AGENCY USE ONLY (Leave Blank)	2. REPORT DATE	3. REPORT TYPE AND DATES COVERED
	July 1996	Final Apr 95 - Apr 96

4. TITLE AND SUBTITLE
FURTHER IMPROVEMENTS ON PLZT BASED MICROSTRUCTURE FOR OPTICAL SWITCHING: A HIGH EFFICIENCY ELECTRO-OPTIC GRATING SWITCH

5. FUNDING NUMBERS
C - F30602-95-C-0102
PE - 62702F
PR - 4600
TA - P4
WU - PR

6. AUTHOR(S)
Q. Wang Song

7. PERFORMING ORGANIZATION NAME(S) AND ADDRESS(ES)
Syracuse University
Office of Sponsored Programs
113 Bowne Hall
Syracuse NY 13244-1200

8. PERFORMING ORGANIZATION REPORT NUMBER
N/A

9. SPONSORING/MONITORING AGENCY NAME(S) AND ADDRESS(ES)
Rome Laboratory/OCPA
25 Electronic Pkwy
Rome NY 13441-4515

10. SPONSORING/MONITORING AGENCY REPORT NUMBER
RL-TR-96-141

11. SUPPLEMENTARY NOTES
Rome Laboratory Project Engineer: Rebecca J. Bussjager/OCPA/(315)330-2918

12a. DISTRIBUTION/AVAILABILITY STATEMENT
Approved for public release; distribution unlimited.

12b. DISTRIBUTION CODE

13. ABSTRACT (Maximum 200 words)

A high diffraction efficiency electro-optic grating switch based on a Lanthanum-modified lead zirconate titanate ceramic wafer is presented. This grating has the advantages of low intrinsic diffraction loss, high zeroth-order light on/off ratio, and fast time response due to employing narrow contour-shaped metal electrodes instead of the commonly used indium tin oxide interdigital electrodes. The zeroth-order light can be turned off with a voltage of 160V.

14. SUBJECT TERMS
PLZT ceramic, Electro-optic grating, Micro-optics, Optical shutter light switch

15. NUMBER OF PAGES
32

16. PRICE CODE

17. SECURITY CLASSIFICATION OF REPORT	18. SECURITY CLASSIFICATION OF THIS PAGE	19. SECURITY CLASSIFICATION OF ABSTRACT	20. LIMITATION OF ABSTRACT
UNCLASSIFIED	UNCLASSIFIED	UNCLASSIFIED	UL

Table of Content

1. Introduction

Interconnections in today's communication system is a very important part. More and more interconnections has become a bottleneck for the developments of such systems. The unique features of optics, such as massive parallel ability and massive free-space interconnections because independent light beams may cross each other without interactions. Electro-optic gratings[1-3] are very useful in many areas where the diffraction efficiency of the grating needs to be controlled by an applied voltage signal, such as programmable optical interconnections and intensity modulators. There are many electro-optic materials we can choose for the construction of electro-optic gratings. A liquid crystal-based electro-optic grating can be operated at a voltage of several volts and achieve a high diffraction efficiency.[4] An electro-optic grating based on solid state crystals such as $LiNbO_3$[5] can also achieve a high efficiency but requires a much higher voltage of several hundred volts. High diffraction efficiency electro-optic gratings can also be used as switches or shutters. They, when properly operated, diffract all of the incident light into higher diffraction orders, thus in essence, switching off the zeroth-order component. In many applications, fast response and long time stability are required. A liquid crystal's slow response and a solid crystal's high operation voltage make them less ideal in some application area.

Lanthanum-modified lead zirconate titanate (PLZT)[6,7] is a polycrystalline ceramic material demonstrating a strong quadratic electro-optic effect at a moderate voltage. Its characteristics of

physical stability, submicrosecond time response and cost-effectiveness has prompted many research efforts for practical applications.[8-20] Using PLZT to fabricate light weight and efficient optical switches/shutters has been an interesting subject.[6,7,17-20] Typically, PLZT based electro-optic shutters use two crossed polarizers to sandwich a PLZT grating whose electrodes are made of metal.[6,7] The orientation of the electrodes bisects the angle made by the two polarizers, i.e., 45° with each of the polarization positions of the two polarizers. When there is no voltage applied on the grating, there is no phase modulation on the light passing through the PLZT, and thus there is no light beyond the second polarizer. When an open voltage is applied, the birefringence effect enables the light polarization to rotate a 90° angle and pass the second polarizer. Electroless plating method[17-18] provides a way to produce low resistance plating electrodes with good characteristics. Half-wave voltage of 190 V was achieved with a response to be within 2 μs. However, the overall transmittance is less than 10%. Using transparent indium tin oxide (ITO) to form the conductive interdigital electrodes, a phase grating structure with high diffraction efficiency was developed.[20] This type of grating takes advantage of the strong phase modulation due to the periodical electrical field. Therefore, it acts as a shutter itself. No polarizer is needed, and a much improved open state transmittance is achieved. It can completely shut off the zeroth-order light with an applied voltage of 140 V thus achieving the purpose of a shutter. The phase distribution of the ITO electrodes, however, forms an intrinsic grating that diffracts part of the incident energy into high orders thus reduces the equivalent transmittance (i.e., the light efficiency) of the switch when no voltage is applied on the device. Reducing the thickness of the ITO electrode is not practical because of the electrical RC time constant considerations. Furthermore, a sheet resistivity below 20 Ω/sq. is considered difficult for sputtering deposition.

In this report we present a performance improved PLZT based high diffraction efficiency grating switch. In addition to improving the light efficiency, this device also employs easy to fabricate, highly conductive narrow contour-shaped metal electrodes instead of commonly used ITO interdigital electrodes. Therefore, it provides a much lower electrical RC time constant, yielding a much improved time response compared to the ITO based grating switch. This grating has the advantages of low intrinsic diffraction loss, whose open state transmittance is much better than the transparent ITO interdigital electrodes based grating switch, high zeroth-order light on/off ratio and fast time response. The zeroth-order light can be turned off with a voltage of 160 V. This report is organized in the following format. In Section 2, the basic electro-optic properties of PLZT is briefed. Design and working principles of the fabricated grating device is presented in Section 3. Section 4 details the fabrication procedure followed by the experimental test of the fabricated device in Section 5. Computer digital simulation of the working principle yields some graphs relating parameters we can choose, which is included in Section 6. In the last section, Section 7, we concludes this report.

2. *Physical and electro-optic properties of PLZT ceramic*

The index of refraction is usually defined as the ratio of the velocity of light in vacuo to the velocity in the medium in question. In a general case there will be two Indices associated with a light propagation direction. The index of refraction of an optical material can be generally expressed in the following mathematical form

$$\left(\frac{1}{n_1^2}\right)x^2+\left(\frac{1}{n_2^2}\right)y^2+\left(\frac{1}{n_3^2}\right)z^2+\left(\frac{1}{n_4^2}\right)yz+\left(\frac{1}{n_5^2}\right)zx+\left(\frac{1}{n_6^2}\right)xy=1. \qquad (2.1)$$

When x, y and z are chosen to be the optical axes of the material the last three terms on the left of the equation will vanish. When a propagation direction is chosen, the two Indices are determined by the two axes of the ellipse which is formed in the interface of the above ellipsoid and a plane normal to the propagation direction. PLZT is polycrystalline, which is prepared from PLZT ponder by hot press in a temperature more than 1000°C. It can be prepared in any size or shape. Without an external field PLZT exhibits an isotopic optical property, with an intrinsic refractive Indices of $n_1 = n_2 = n_3 = n_0 = 2.5$, and $n_4 = n_5 = n_6 = 0$. That is

$$x^2+y^2+z^2=n_0^2. \qquad (2.2)$$

PLZT ceramic is quite transparent for a large range of wavelength. But due to its high intrinsic refractive index PLZT wafer has an intrinsic transmittance of 67% caused by its surface reflections.[12] With proper anti-reflection coating on the surface, the transmittance can be increased as high as 98%.

PLZT has large quadratic electro-optic coefficients. When PLZT is placed in a spatially distributed electrical field, its index of refraction changes according to the following principle

$$\begin{bmatrix} \Delta\left(\frac{1}{n_1^2(x,y,z)}\right) \\ \Delta\left(\frac{1}{n_2^2(x,y,z)}\right) \\ \Delta\left(\frac{1}{n_3^2(x,y,z)}\right) \\ \Delta\left(\frac{1}{n_4^2(x,y,z)}\right) \\ \Delta\left(\frac{1}{n_5^2(x,y,z)}\right) \\ \Delta\left(\frac{1}{n_6^2(x,y,z)}\right) \end{bmatrix} = \begin{bmatrix} R_{11} & R_{12} & R_{12} & 0 & 0 & 0 \\ R_{12} & R_{11} & R_{12} & 0 & 0 & 0 \\ R_{12} & R_{12} & R_{11} & 0 & 0 & 0 \\ 0 & 0 & 0 & R_{44} & 0 & 0 \\ 0 & 0 & 0 & 0 & R_{44} & 0 \\ 0 & 0 & 0 & 0 & 0 & R_{44} \end{bmatrix} \begin{bmatrix} E_x^2(x,y,z) \\ E_y^2(x,y,z) \\ E_z^2(x,y,z) \\ E_y(x,y,z)E_z(x,y,z) \\ E_z(x,y,z)E_x(x,y,z) \\ E_x(x,y,z)E_y(x,y,z) \end{bmatrix}, \tag{2.3}$$

where (x,y,z) denotes the location inside the substrate, R_{ij} indicates the quadratic electro-optic (Kerr) coefficients. When taking the electrical field direction as the x'-axis of a transformed coordinate system, the index change can be approximately simplified as

$$\Delta n_{x'}(x,y,z) = -\frac{1}{2} n_0^3 R_{11} E^2(x,y,z), \tag{2.4}$$

$$\Delta n_{y'}(x,y,z) = -\frac{1}{2} n_0^3 R_{12} E^2(x,y,z), \text{ and} \tag{2.5}$$

$$\Delta n_{z'}(x,y,z) = -\frac{1}{2} n_0^3 R_{12} E^2(x,y,z), \tag{2.6}$$

where $\Delta n_{x'}$, $\Delta n_{y'}$ and $\Delta n_{z'}$ refer to the refractive index changes when the polarization of the light is parallel to the electrical field direction and the other two perpendicular to the electrical field and each other. Thus the induced refractive indices are

$$n_{x'}(x,y,z) = n_0 - \frac{1}{2} n_0^3 R_{11} E^2(x,y,z), \tag{2.7}$$

$$n_{y'}(x,y,z) = n_{z'}(x,y,z) = n_0 - \frac{1}{2} n_0^3 R_{12} E^2(x,y,z). \tag{2.8}$$

The refractive index ellipsoid is expressed

$$\left(\frac{1}{n_{x'}^2(x,y,z)}\right)x'^2+\left(\frac{1}{n_{y'}^2(x,y,z)}\right)y'^2+\left(\frac{1}{n_{z'}^2(x,y,z)}\right)z'^2=1. \tag{2.9}$$

For the polarization which makes an arbitrary angle, $\theta(x,y)$, with the applied electrical field the refractive index change can be deduced by the following formula

$$\frac{1}{n^2(\theta(x,y))}=\frac{\cos^2(\theta(x,y))}{n_x^2(x,y)}+\frac{\sin^2(\theta(x,y))}{n_z^2(x,y)}. \tag{2.10}$$

PLZT's electro-optic coefficient can be different if the lanthanum concentration changes. As in our case PLZT 9/65/35 was used. This material has a 65/35 ratio of $PbZrO_3$ to $PbTiO_3$ with a lanthanum concentration of 9%. Numerical values of the Kerr coefficients in the literature[12-13] are

$$R_{11}=4.00\times10^{-16}\left(\frac{m^2}{V^2}\right), \tag{2.11}$$

$$R_{12}=-2.42\times10^{-16}\left(\frac{m^2}{V^2}\right). \tag{2.12}$$

3. Device design and principles

To design a device, we should use as maximum effect mentioned above as possible. Our design of the PLZT-based high efficient electro-optic grating is illustrated in Figure 1.

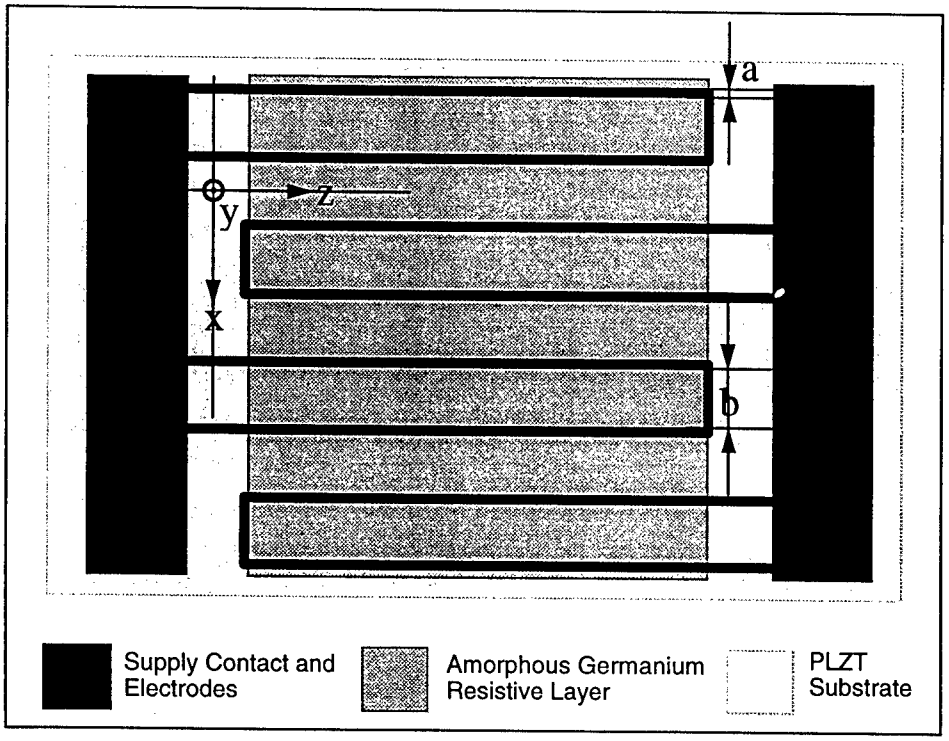

Figure 1. Electro-optic grating based on PLZT ceramic.

Figure 1 illustrates the top view of the designed electro-optic grating. All fabricated elements are on the top side of the wafer surface. The structure consists of narrow metal outlines of the interdigital electrodes and a transparent resistive layer. The outlines are illustrated in the figure by black lines, which have a width of *a*. The transparent parts other than the outlines, which have a width of *b*, will allow light to pass. The area surrounded by a closed metal outline is equivalent to an electrode. It has a uniform potential distribution. The area between the adjacent closed metal lines is defined as the space. It has a linear potential distribution along the direction normal to the electrodes (i.e., *x* direction). The light experiences a phase modulation determined by the voltage between two neighboring electrode outlines. The ratio, $a/(a+b)$, determines the blocked light and intrinsic diffraction loss. To ensure a good light utility, the electrode outlines should be made as narrow as possible but sufficient for a high conductivity. In other words, a compromise between

light utility and RC time constant needs to be considered. Electrically, the device can be viewed as a lossy capacitor. Previous research[21] found that the electron concentration is much higher at the edge than any other parts on an electrode. The edge, from an electrical point of view, has an important role in maintaining the potential distributions on the electrodes. So a conductive outline functions as if the enclosed area is covered with a conductive layer and provides high conductivity to reduce the charging time of the intrinsic capacitor of the device. A resistive layer is used over the entire working area of the PLZT substrate, the purpose of the layer is to provide a bias resistance that promises the surface potential distribution inside the electrode outlines to be uniform and the potential distribution between electrodes to be linear. The resistivity is chosen to be as large as possible to minimize the power consumption while the above mentioned effect is maintained.

PLZT is a tetragonal material displaying optically uniaxial properties. Because the device we proposed is basically of one-dimensional distribution, so that the field distribution and the induced refractive index distribution inside the substrate is two-dimensional expressible, i.e., function of (x,y). When a voltage is applied on the grating, the field dependent indices inside the PLZT substrate are given by

$$n_x(x,y) = n_0 - \frac{n_0^3}{2}\left[R_{11}E_x^2(x,y) + R_{12}E_y^2(x,y)\right], \tag{3.1}$$

$$n_z(x,y) = n_0 - \frac{n_0^3}{2}R_{12}\left[E_x^2(x,y) + E_y^2(x,y)\right], \tag{3.2}$$

where n_x and n_z denote the indices for the light polarized along x and z axises, respectively. E_x and E_y are the electrical field components induced, and R_{11} and R_{12} are the quadratic electro-optic coefficients of the PLZT. For the region beneath an electrode, the E_y component is larger than E_x.

While in the region beneath a space, E_x is larger than E_y. Thus a different signed n_x change results for these two cases because of the different signs bore by R_{11} and R_{12}, and hence, a larger modulation of the index n_x than n_z is produced. An x-polarized light beam will require lower voltage than that of the z-polarized light for this grating.

We assume that the dimensions of the working area of the grating in both x and z are far larger than a and b. The modulation of the grating can be divided into two parts, amplitude and phase modulations. Phase modulation is caused by the electro-optic effect and amplitude by the opaque nature of the metal electrode outlines. According to Figure 1, the amplitude or intensity transmittance modulation is given by

$$T(x,0)=\begin{cases}1, & \left(-\frac{b}{2}\le x<\frac{b}{2}\right),\\ 0, & \left(\frac{b}{2}\le x<\frac{b}{2}+a\right),\end{cases} \quad \text{and} \tag{3.3}$$

$$T(x+a+b,0)=T(x,0). \tag{3.4}$$

The phase modulation can be obtained by tracing the electro-optic effects inside the substrate. First let us consider the boundary condition. The boundary condition for the voltage distribution on the top surface of the PLZT wafer is given by

$$V(x,0)=\begin{cases}\frac{V_0}{b}x, & \left(-\frac{b}{2}\le x<\frac{b}{2}\right),\\ \frac{V_0}{2}, & \left(\frac{b}{2}\le x<\frac{3b}{2}+2a\right),\end{cases} \quad \text{and} \tag{3.5}$$

$$V(x+2a+2b,0)=-V(x,0), \tag{3.6}$$

where V_0 is the voltage applied over the electrodes. The situation is illustrated in Figure 2.

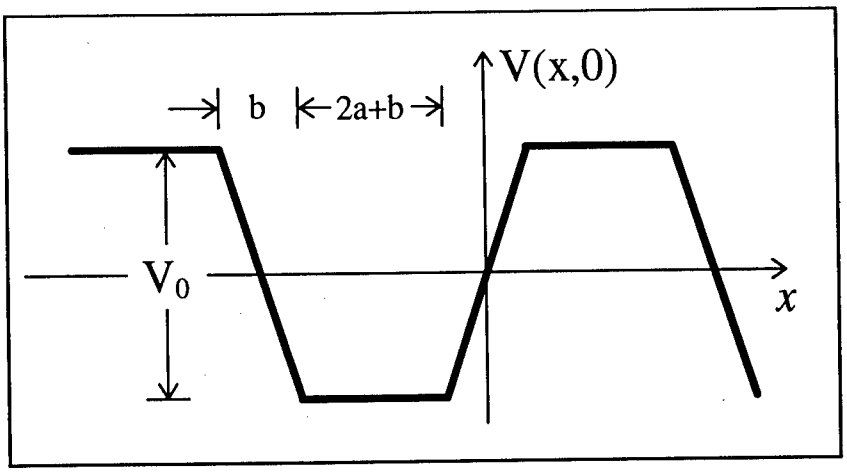

Figure 2. Boundary condition of voltage distribution.

Because all the electrodes are on the top surface of the electro-optic substrate, the electrical field exponentially decays along the y direction and becomes negligible when y is very large. The periodical form of the boundary condition suggests a general form of the potential distribution inside the PLZT substrate in terms of Fourier components of the top surface boundary condition,

$$V(x,y)=\sum_{n=1}^{\infty} P(\xi_n)\sin(\xi_n x)\exp(-\xi_n y), \tag{3.7}$$

where

$$\xi_n=\frac{n\pi}{2(a+b)}, \qquad (n=1, 2, \ldots, \infty), \tag{3.8}$$

$$P(\xi_n)=\frac{1}{a+b}\int_0^{2(a+b)} V(x,0)\sin(\xi_n x)dx\,. \tag{3.9}$$

ξ_n is the nth angular spatial frequency and $P(\xi_n)$ is the nth Fourier component of the boundary condition expressed by Eqs. (3.5) and (3.6). The electrical field distribution can be obtained by taking gradient to the potential distribution

$$E_x(x,y) = -\frac{\partial V(x,y)}{\partial x} = -\sum_{n=1}^{\infty} \xi_n P(\xi_n) \cos(\xi_n x) \exp(-\xi_n y), \tag{3.10}$$

$$E_y(x,y) = -\frac{\partial V(x,y)}{\partial y} = \sum_{n=1}^{\infty} \xi_n P(\xi_n) \sin(\xi_n x) \exp(-\xi_n y). \tag{3.11}$$

Thus the electrically changeable refractive-indices can be found by Eqs. (3.1) and (3.2). Suppose a normal incident of the illuminating light, we have the phase modulations for x- and z-polarized light written as

$$\phi_x(x) = \frac{2\pi}{\lambda} \int_0^t n_x(x,y) dy, \tag{3.12}$$

$$\phi_z(x) = \frac{2\pi}{\lambda} \int_0^t n_z(x,y) dy, \tag{3.13}$$

here, t is the thickness of the PLZT substrate. Combining the amplitude and phase modulations, we have the optical modulation expression for the grating. A Fourier transform on it yields a diffraction pattern. The intensity of different diffraction can then be obtained.

4. Device fabrication issues

Fabrication was performed on a PLZT 9/65/35 ceramic wafer of size 15mm×15mm×0.32mm. An amorphous germanium layer of 11nm thick was thermally evaporated onto the substrate as a bias resistive sheet, yielding a sheet resistivity higher than 3800 MΩ/sq. Chromium/aluminum electrode outlines were then thermally evaporated on the germanium layer through an image reversal and wet lift-off process. The aluminum layer was evaporated to be 300nm thick. This gave the metal lines a sheet resistivity below 0.2 Ω/sq. or an equivalent electrode sheet resistivity

below 3 Ω/sq. if we treat the electrode outline and the space it surrounded as a uniform electrode. The fabricated grating has a working area of 7.5mm × 5mm. Electrodes were made to have a period of 0.2 mm with the width of the opaque metal outline to be 4μm.

5. Experimental test of the device

To perform the experimental test, a linearly polarized He-Ne laser beam of 633nm with its axis normal to the device surface was incident onto the electro-optic grating. A high voltage power supply was used to generate a step-function voltage signal as large as 160 V. The incident beam was polarized in the *x* direction as indicated in Figure 1. The transmitted beam was examined at a distance of about one meter behind the device.

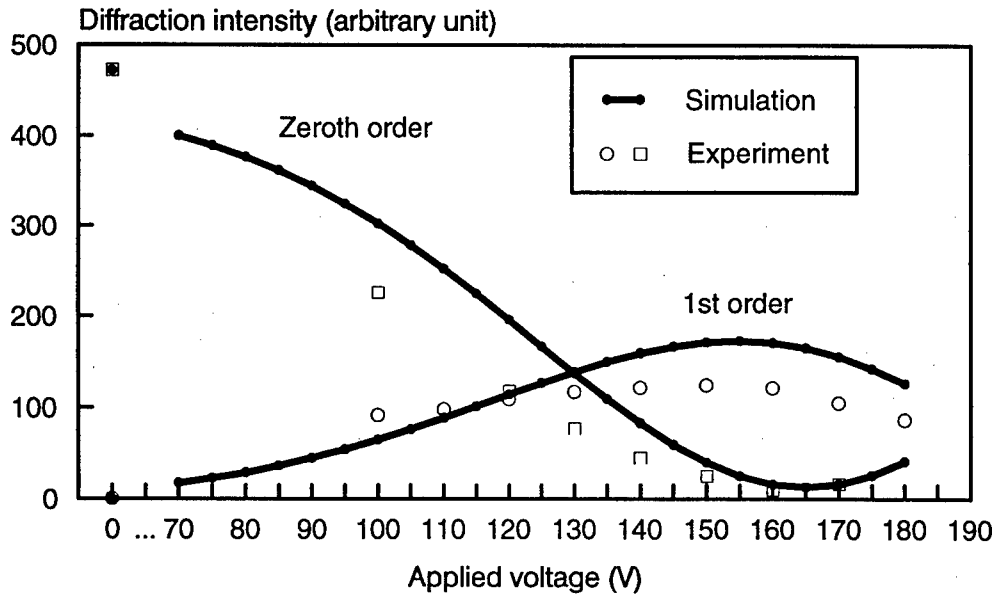

Figure 3. Relationship of diffraction order intensities and applied voltages.

Figure 3 shows the measured relationship of the zeroth-order and first-order diffraction intensities versus the applied voltage, plotted by squares and circles, respectively. To compare with the theoretical predictions, computer simulation results, which will be explained later in the report, are also plotted on this graph by dotted solid curves. The experimentally measured intensities were normalized by the simulated value when no voltage is applied, because this value largely depends on the number of points selected for the fast Fourier transform. The shut-off state was achieved at an applied voltage of 160 V. At the dark/shut-off state, the zeroth-order light is less than 0.7% of the incident light. Because of the electrode outlines' layout, the intrinsic grating structure has a period half as much as the period of the electro-optically induced grating. So the first order diffraction of the electro-optic grating does not appear when no voltage is applied. So next to the zeroth order, it is the second diffraction order or, in another name, the first order of the electrode outline diffraction. It should be stated that this device permitted a high transmittance when there is no external voltage applied. The total transmittance of the device is 35%, in which the zeroth-order takes 92% of it. The device we fabricated looks like a plain wafer with unnoticeable diffraction. It can be further improved. The PLZT ceramic wafer has a refractive index of 2.5 and thus an intrinsic transmittance of 67% due to its surface reflections.[7] With proper anti-reflection coating on the surface, the transmittance of the wafer can be increased as high as 98%.

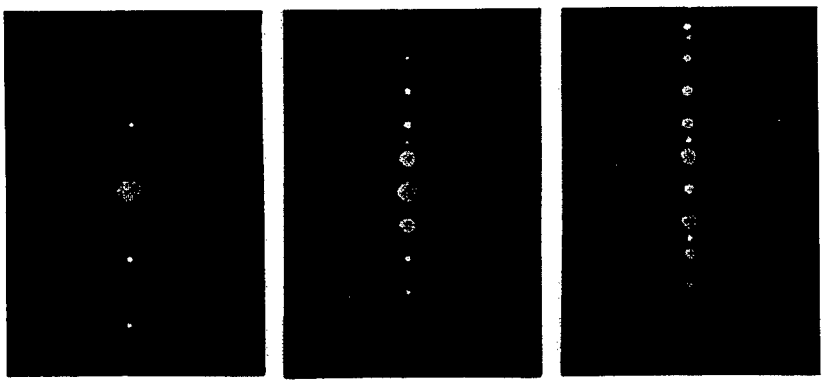

a) b) c)

Figure 4. Diffraction pattern with a) no applied voltage, b) 100 V, and c) 160 V.

The shut-off ratio, i.e. the ratio of zero-order intensity without power applied to the one with 160 V applied voltage, was measured over 48 to 1. Figure 4 shows the photos of the diffraction patterns. Figure 4(a) is with no applied voltage, Figure 4(c) is with the shut-off voltage applied, and Figure 4(b) is a case in between. The zeroth-order in Figure 4(c) appears bright in photo than what it really is because of the film's logarithmic response. The shut-off voltage of 160 V reported here is higher than the formerly achievement voltage of 140 V. This is due to the ITO[20] intrinsic grating structure made in previous fabrication, where the ITO grating electrodes make about 30% of the bias of the phase grating. The grating structure here, however, is totally induced by the 160 V shut-off voltage. The zeroth-order transmittance makes most of the transmitted light. We used amorphous germanium for the resistive layer because of fabrication convenience. This material absorbed light and decreased the light utility. An amorphous silicon layer[22] would be more transparent and thus may produce better result. The zeroth-order transmittance can be increased by optimizing the layout of the design, such as a better resistive layer deposit and an

anti-reflection coating. The light utility can thus be dramatically improved to the value close to $b/(a+b)$ which is > 96% in our case.

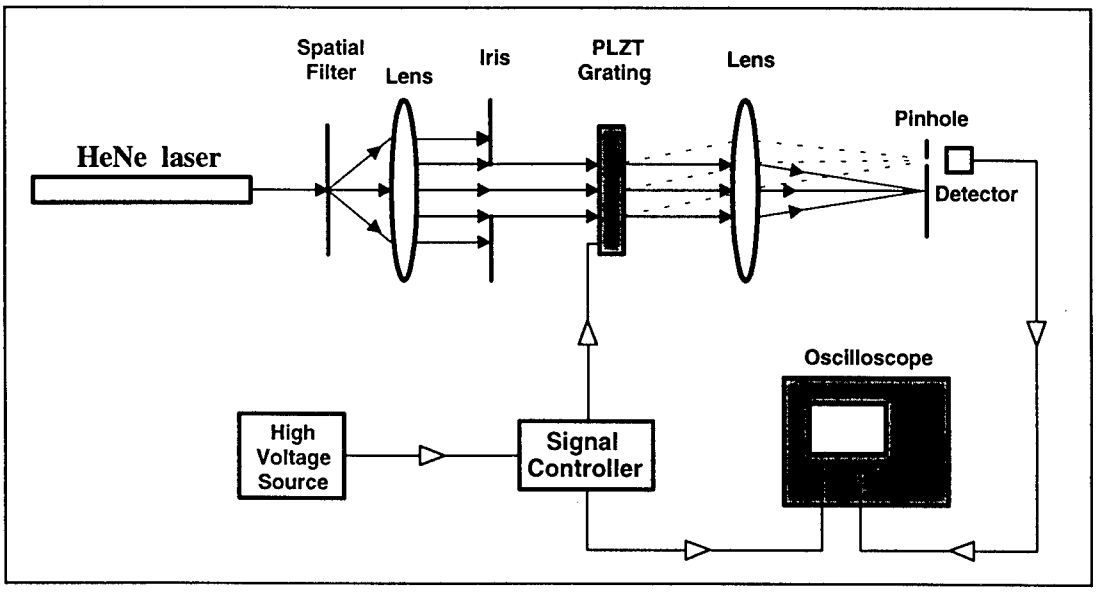

Figure 5. Time response measurement setup.

The time response is another parameter to judge the performance of the device for application. To measure the time response of the device, we set up a system as shown in Figure 5. The photodetector can respond to a signal frequency up to 3GHz. The power supply can generate a step voltage signal, the risetime of the source signal is within 2μs. We also monitored the temporary current flow through the grating electrodes after the step voltage is put on. The time between the initialization and the vanish of the charging current is 18μs. And the measured time response from the beam spot is 6μs.

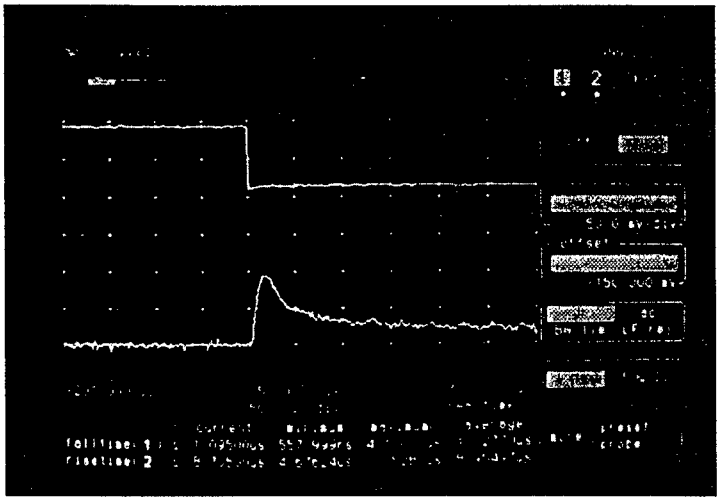

Figure 6. Photo of the time response displayed on an oscilloscope.

Figure 6 gives a typical response signal display on a Hewlett Packard 54510A Digitizing Oscilloscope. This time response is of two orders of magnitude faster than that of the ITO interdigital grating. The resistance of the metal outlines can be further decreased by increasing the metal lines deposition thickness or using a more conductive metal like copper or gold, thus yielding a decrease in response time.

6. Computer simulations

Computer simulation was performed by using the coefficients previously mentioned. Fourier components decomposition and weighted composition with the fast Fourier transform method was used for the determination of the potential distributions inside the PLZT wafer. Electrical

field followed by index changes were determined by following the common procedures as defined in Section 3.

The simulation gives a shut-off voltage of 165 V, as shown by a solid curve in Figure 3. Although the simulated results do not fit the experimental results exactly, they do have the same trends and a very similar shut-off voltage. We contribute the difference to the charge concentration on the PLZT surfaces because of PLZT's large dielectric constant, which were not considered in numerical simulations. We also simulated the dependence of the shut-off voltage on the grating period. Results are shown in Figure 7.

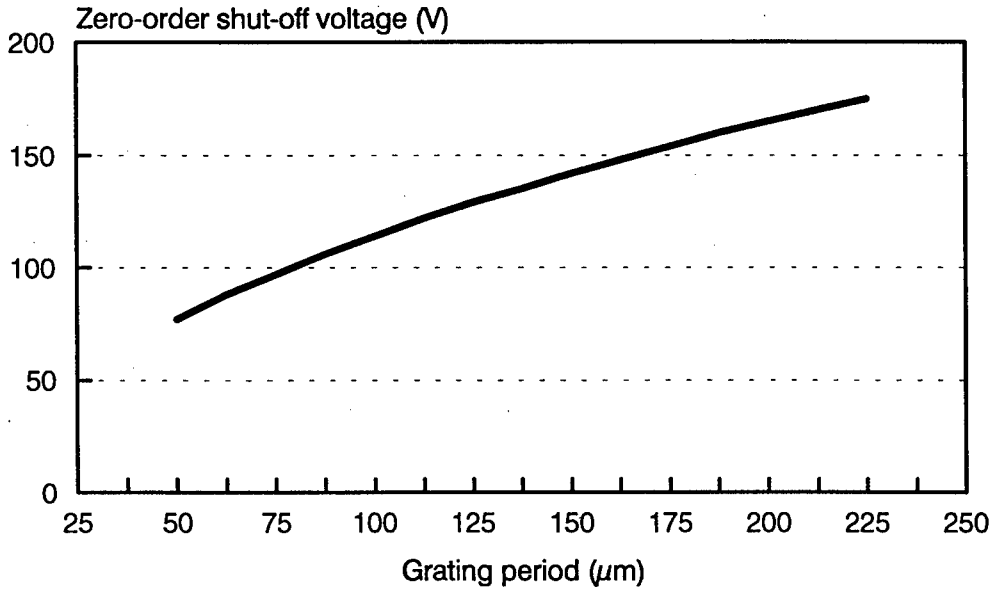

Figure 7. Simulated relationship of zero-order shut-off voltage versus grating period.

Generally the shut-off voltage decreases as the grating period decreases. But, on the other hand, the electrical field intensity increases, too. Taking in mind the potential damage to the PLZT at a high electrical field, the grating period cannot be too short.

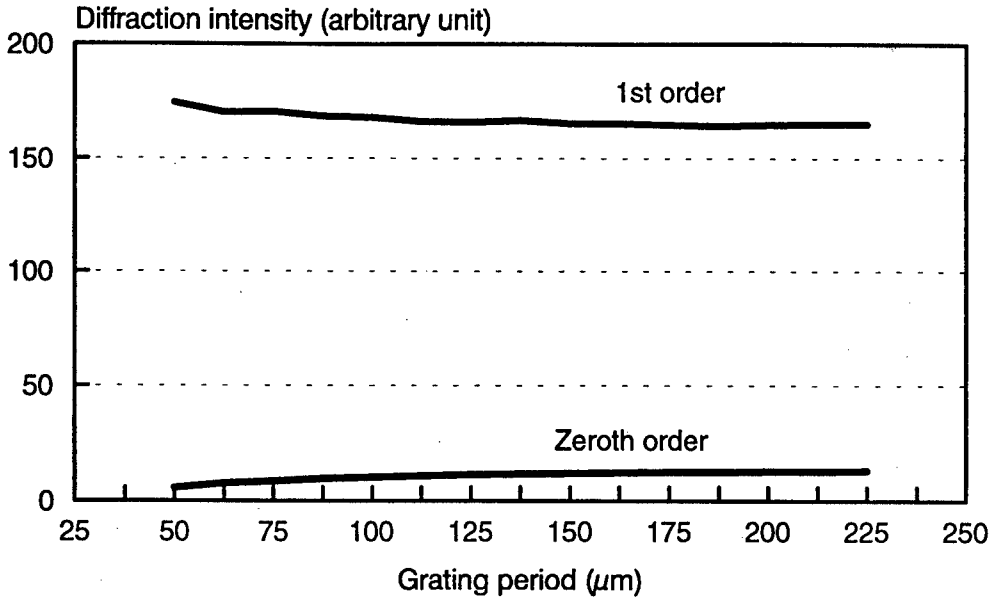

Figure 8. Simulated relationships between diffraction intensities and grating period at zero-order shut-off voltage.

Figure 8 gives the simulated diffraction efficiencies of the grating at shut-off voltages for different grating periods. It shows that the smaller the period, the higher the shut-off ratio. So the thickness of the wafer substrate does influence the performance of the grating. Although the grating uses transverse electro-optic effect, and the electrical field is predominately near the surface where the electrodes are, the field does not vanish at the bottom surface of the substrate. The smaller the period is, the weaker the field near the bottom surface is. From the figure, we can say to some extent that a thicker PLZT substrate (in measurement of thickness/grating-period) will have a better grating performance. If the substrate were thick enough so that the electrical field near the bottom surface is negligible for any reasonable grating period, the curves in this figure would

remain straight and parallel to the horizontal axis because of the similarity of the electrical field distribution for different grating periods.

7. Discussions and Conclusions

In conclusion, an electro-optic grating with improved performance based on a substrate of PLZT ceramic has been demonstrated. The design takes the outline of the original ITO based interdigital layout and uses conductive metals to make the outlines. As a result, the intrinsic resistance of the electrode and the intrinsic diffraction loss due to the electrodes are reduced dramatically. High light transmittance and fast time response have been observed. With this design, the electrode's resistance is no longer a restriction for the time response of the device.

References:

1. J. M. Hammer, "Digital electro-optic grating deflector and modulator," Appl. Phys. Lett. **18**, 147-149 (1971).
2. H. Sato and K. Toda, "A new electrically controllable diffraction grating using polarization reflection," J. Appl. Phys. **47**, 4031-4032 (1976).
3. T. Utsunomiya and H. Sato, "Electrically deformable diffraction grating using a piezoelectric material," Ferroelectrics, **27**, 27-30 (1980).
4. T. J. Chen, P. J. Bos, H. Vithana, and D. L. Johnson, "An electro-optically controlled liquid crystal diffraction grating," Appl. Phys. Lett. **67**, 2588-2590 (1995).
5. R. T. Chen, D. Robinson, H. Lu, M. R. Wang, T. Jannson, and R. Baumbick, "Reconfigurable optical interconnection network for multimode optical fiber sensor arrays," Opt. Eng. **31**, 1098-11106 (1992).
6. G. H. Haertling, "PLZT electrooptic ceramics and devices," in *Industrial Applications of Rare Earth Elements*, K. A. Gschneidner, Jr. Ed., ACS Symposium Series, **164**, 265-283 (1981).
7. G. H. Haertling, "Piezoelectric and electrooptic ceramics," in *Ceramic Materials for Electronics: Processing, Properties, and Applications,* R. C. Buchanan Ed., (1986) Marcel Decker, Inc. New York and Basel, 139-225.
8. Q. Wang Song, X.-M. Wang, R. Bussjager, and J. Osman, "Electro-optic beam steering device based on PLZT ceramic wafer," to appear in *Applied Optics.*

9. J. A. Thomas and Y. Fainman, "Programmable diffractive optical element using a multichannel lanthanum-modified lead zirconate titanate phase modulator," Opt. Lett. **20**, 1510-1512 (1995).

10. C. E. Land and P. S. Peercy, "Ion-implanted PLZT for photoferroelectric image storage and display device," Ferroelectrics, **27**, 131-136 (1980).

11. C. E. Land and P. S. Peercy, "Photosensitivity enhancement by H- and He-ion implantation in lead lanthanum zironate titanate ceramics," Appl. Phys. Lett. **37**, 39-41 (1980).

12. J. T. Cutchen, "PLZT thermal/flash protective goggles: device concepts and constraints," Ferroelectrics, **27**, 173-178 (1980).

13. H. Sato, T. Tatebayashi, T. Yamamoto, and K. Hayashi, "Electro-optic lens composed of transparent electrodes on PLZT ceramic towards optoelectronic devices," in *Optics in Complex Systems*, F. Lanzl, H. Preuss, and G. Weigelt, Eds., Proc. Soc. Photo-Opt. Instrum. **1319**, 493-494 (1990).

14. T. Tatebayashi, T. Yamamoto, and H. Sato, "Electro-optic variable focal-length lens using PLZT ceramic," Appl. Opt. **30**, 5049-5055 (1991).

15. T. Tatebayashi, T. Yamamoto, and H. Sato, "Dual focal point electro-optic lens with a Fresnel-zone plate on a PLZT ceramic," Appl. Opt. **31**, 2770-2775 (1992).

16. Q. Wang Song, X.-M. Wang, and R. Bussjager, "PLZT ceramic wafer based electro-optic dynamic diverging lens," Optics Letters, (In Press, 1996).

17. K. Nagata and H. Honma, "Properties of PLZT shutter with copper plating electrodes," Jpn. J. Appl. Phys. Suppl. **28-2**, 167-169 (1989).

18. K. Nagata, "PLZT optical shutter with copper electrodes by electroless plating," Ferroelectrics, **109**, 247-252 (1990).

19. T. Utsunomiya, "Optical switch using PLZT ceramics," Ferroelectrics, **109**, 235-240 (1990).

20. Q. Wang Song, P. J. Talbot, and J. H. Maurice, "PLZT based high-efficiency electro-optic grating for optical switching," J. Mod. Opt. **41**, 717-727 (1994).

21. M. A. Title and S. H. Lee, "Modeling and characterization of embedded electrode performance in transverse electrooptic modulators," Appl. Opt. **29**,85-98 (1990).

22. A. Riza and M. C. DeJule, "Three-terminal adaptive nematic liquid-crystal lens device," Opt. Lett. **19**, D. 1013-1015 (1994).

91

*U.S. GOVERNMENT PRINTING OFFICE: 1996-710-126-47026

MISSION

OF

ROME LABORATORY

Mission. The mission of Rome Laboratory is to advance the science and technologies of command, control, communications and intelligence and to transition them into systems to meet customer needs. To achieve this, Rome Lab:

a. Conducts vigorous research, development and test programs in all applicable technologies;

b. Transitions technology to current and future systems to improve operational capability, readiness, and supportability;

c. Provides a full range of technical support to Air Force Materiel Command product centers and other Air Force organizations;

d. Promotes transfer of technology to the private sector;

e. Maintains leading edge technological expertise in the areas of surveillance, communications, command and control, intelligence, reliability science, electro-magnetic technology, photonics, signal processing, and computational science.

The thrust areas of technical competence include: Surveillance, Communications, Command and Control, Intelligence, Signal Processing, Computer Science and Technology, Electromagnetic Technology, Photonics and Reliability Sciences.